Model Identification of Marine Robots

Project Overview

Understanding and modeling the dynamics of marine robots is critical for developing accurate control strategies, improving maneuverability, and ensuring robust operation in real-world conditions. Realistic models enable simulation-based design, controller testing, and performance prediction without costly or risky field experiments. Through hands-on identification, you will gain practical insight into the challenges of translating theory into reliable models that reflect real vehicle behavior.

In this project, you will:

1. **Acquire Experimental Data** – Collect motion and force measurements from an Autonomous Surface Vehicle (ASV) using sensors and a predefined excitation trajectory.
2. **Develop Model-Identification Code** – Implement algorithms in MATLAB, Python, C, or another suitable language to estimate the dynamic parameters of the ASV model.
3. **Perform ASV Model Identification** – Use the acquired data and your code to identify key hydrodynamic coefficients and inertia terms.
4. **Analyze and Compare Results** – Validate your identified model against the experimental data, then compare the outcomes with those presented in the reference paper [1]. Highlight key similarities and differences, and discuss possible sources of error or uncertainty.

Autonomous Surface Vehicle Dynamics

The ASV (shown in Fig. 1) measures 0.90 m in length, 0.45 m in width, 0.14 m in height, and weighs 15 kg. The ASV features four thrusters positioned around the hull (Fig. 2), allowing for holonomic motion. The computing system has an Intel NUC 13 Pro Kit Mini Computer with 32 GB of RAM, selected for its compact size, lightweight, and high computational capacity. We use a Velodyne VLP-32C LiDAR, paired with a Microstrain 3DM-GX5-25 Inertial Measurement Unit (IMU) to perform real-time LiDAR Inertial Odometry [2], achieving centimeter-level localization accuracy. The NUC sends force commands to a STM 32 microcontroller, which translates them into PWM signals for the BlueRobotics T100 Thrusters. Following the notation developed by Fossen [3], the dynamics of a USV can be generically described by the nonlinear differential equation

$$\mathbf{M}\dot{\mathbf{v}} + \mathbf{C}(\mathbf{v})\mathbf{v} + \mathbf{D}(\mathbf{v})\mathbf{v} = \boldsymbol{\tau} \tag{1}$$

where $\mathbf{v} = [u\ v\ r]^T$ denotes the vehicle velocity, which contains the vehicle surge velocity (u), sway velocity (v), and yaw rate (r) in the body fixed frame, $\mathbf{M} \in \mathbb{R}^{3\times3}$ is the positive-definite symmetric added mass and inertia matrix, $\mathbf{C}(\mathbf{v}) \in \mathbb{R}^{3\times3}$ is the skew-symmetric vehicle matrix of Coriolis and centripetal terms, $\mathbf{D}(\mathbf{v})$ is the positive-semi-definite drag matrix-valued function, $\boldsymbol{\tau} \in \mathbb{R}^{3\times1}$ the vector of body-frame forces and moments applied to the vehicle in all three DOFs and $\boldsymbol{\tau} = [\tau_1\ \tau_2\ \tau_3]^T$. Fig. 2 illustrates the two coordinate systems and the thruster forces acting on the vehicle.

We define $\boldsymbol{\eta} = [x\ y\ \psi]^T$ as the position and orientation of the robot in the inertial frame, relative to the center of mass. The kinematic equation relating velocity components in the inertial frame to those in the body frame is described as

$$\dot{\boldsymbol{\eta}} = \mathbf{R}(\psi)\mathbf{v} \tag{2}$$

where $\mathbf{R}(\psi)$ is the transformation matrix converting a state vector from body frame to inertial frame

$$\mathbf{R}(\psi) = \begin{bmatrix} \cos\psi & -\sin\psi & 0 \\ \sin\psi & \cos\psi & 0 \\ 0 & 0 & 1 \end{bmatrix} \tag{3}$$

Figure 1: The ASV prototype navigating on a lake.

The decoupled symmetric mass matrix is $\mathbf{M}$, where $\mathbf{M} \in \mathbb{R}^{3\times 3}$ is the sum of the vehicle mass and added mass matrix

$$\mathbf{M} = \text{diag}\{m_{11}, m_{22}, m_{33}\} \tag{4}$$

The matrix $\mathbf{C}(\mathbf{v})$ also contains the rigid-body matrix and the added mass matrix. Considering that the origin O_b coincides with the center of mass of the robot, i. e., $x_G = 0$ and $y_G = 0$, $\mathbf{C}(\mathbf{v})$ can be expressed as

$$\mathbf{C}(\mathbf{v}) = \begin{bmatrix} 0 & 0 & -m_{22}v \\ 0 & 0 & m_{11}u \\ m_{22}v & -m_{11}u & 0 \end{bmatrix} \tag{5}$$

Since our robot is always moving at low speeds, the drag matrix $\mathbf{D}(\mathbf{v})$ is represented by a linear damping term. Moreover, because the platform is designed to be symmetrical with respect to the x_b and y_b axes in the body-fixed frame, the following form of the drag matrix is adopted

$$\mathbf{D}(\mathbf{v}) = \text{diag}\{X_u, Y_v, N_r\} \tag{6}$$

Further, the applied force and moment vector $\boldsymbol{\tau}$ can be written as

$$\boldsymbol{\tau} = \mathbf{B}\mathbf{u} = \begin{bmatrix} 1 & 1 & 0 & 0 \\ 0 & 0 & 1 & 1 \\ \frac{a}{2} & -\frac{a}{2} & \frac{b}{2} & -\frac{b}{2} \end{bmatrix} \begin{pmatrix} f_1 \\ f_2 \\ f_3 \\ f_4 \end{pmatrix} \tag{7}$$

where $\mathbf{B}$ is the control matrix describing the thruster configuration and $\mathbf{u}$ is the control vector. a is the distance between the transverse propellers and b is the distance between the longitudinal propellers, f_1, f_2, f_3 and f_4 are the forces generated by the corresponding propellers, as shown in Fig. **??**. Each propeller is fixed and can generate forward and backward forces. Finally, Eqn. 1 and 2 can be written as

$$\dot{\boldsymbol{\eta}} = \mathbf{R}(\psi)\mathbf{v} \tag{8}$$

$$\dot{\mathbf{v}} = \mathbf{M}^{-1}\mathbf{B}\mathbf{u} - \mathbf{M}^{-1}(\mathbf{C}(\mathbf{v}) + \mathbf{D}(\mathbf{v}))\mathbf{v} \tag{9}$$

The complete dynamic model of the surface vehicle is reformulated by combining Eqs. (8) and (9), given by

$$\dot{\mathbf{q}} = f(\mathbf{q}, \mathbf{u}) \tag{10}$$

where $\mathbf{q} = [x\ y\ \psi\ u\ v\ r]^T$ is the state vector of the robot.

Model Identifacation Problem Formulation and Alternative Solutions

The ASV dynamics are represented using a **grey-box model** with unknown hydrodynamic parameters. The parameters to be estimated include the mass coefficients m_{11}, m_{22}, and m_{33}, as well as the drag coefficients X_u, Y_v, and N_r. The parameter identification can be formulated as the following constrained optimization problem:

$$\begin{aligned} &\arg\min_{\lambda} \ \textstyle\sum_t \varepsilon(t)^T W \varepsilon(t), \\ &\text{s.t.} \ \lambda_l \leq \lambda \leq \lambda_u \end{aligned} \tag{11}$$

Here, $\varepsilon(t)$ represents the velocity error between the experimental measurement $U_e(t)$ and the simulated velocity $U_s(t)$:

$$\varepsilon(t) = U_e(t) - U_s(t), \tag{12}$$

$\lambda = \{m_{11}, m_{22}, m_{33}, X_u, Y_v, N_r\}$ is the parameter vector to be estimated, while λ_l and λ_u are the respective lower and upper bounds. The diagonal weight matrix W assigns relative importance to each velocity component during optimization. A grey-box identification algorithm [4] can be applied, and the problem can be solved numerically using a nonlinear least-squares method, such as the trust-region reflective algorithm. Model details of the model identification process and results can be found in [1].

Alternative Solution Ideas

1. **Bayesian Parameter Estimation** Use a Bayesian framework to incorporate prior knowledge of hydrodynamic parameters and quantify parameter uncertainty. Techniques such as Markov Chain Monte Carlo (MCMC) or variational inference can provide posterior distributions rather than single point estimates.

2. **Machine Learning-Based Regression** Use neural networks or Gaussian process regression to approximate hydrodynamic forces from input-output data. Combine these black-box models with known physics for a hybrid grey-box approach.

3. **Recursive or Online Identification** Implement an online adaptive scheme such as Recursive Least Squares (RLS) or Extended Kalman Filter (EKF) to update parameter estimates in real time as new data is acquired.

4. **Regularization Techniques** Introduce L1/L2 penalties on λ to prevent overfitting and improve generalization, especially if experimental data are noisy or limited.

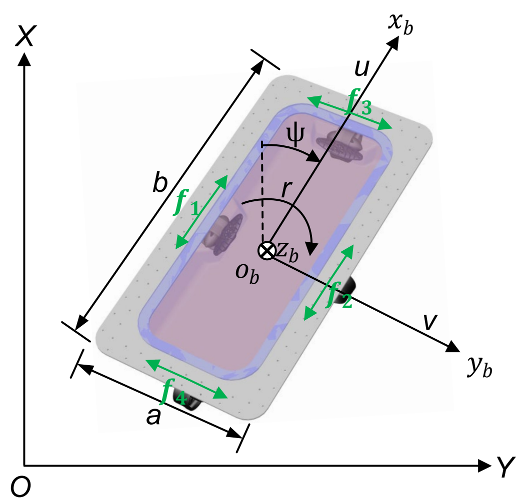

Figure 2: The ASV coordinate system with four thrusters positioned on each side of the robot. Each thruster generates both forward and reverse forces.

Data Collection for Identification

The identification dataset was collected while the robotic boat was commanded to follow a sinusoidal trajectory in a swimming pool. This excitation induced coupled motion in the surge, sway, and yaw degrees of freedom.

During the experiments, the input forces f_1, f_2, f_3, and f_4, along with the corresponding robot states x, y, ψ, u, v, and r, were recorded at a sampling rate of 10 Hz. The sinusoidal trajectory had an amplitude of 0.8 m and a frequency of 0.05 Hz (amplitude and frequency subject to change).

Students are first advised to manually collect five trials to gain familiarity with the procedure. Afterwards, the TA will assist in automating the sinusoidal path-following commands. A total of ten trials is recommended to ensure data redundancy, address potential recording issues, and assess the consistency of the model identification.

Due Date

October 2, 2025

Deliverables

1. In-Class Presentation (October 2, 2025): 10–15 minutes
2. Written Report (October 2, 2025): 2–3 pages, formatted using LaTeX

References

[1] W. Wang, L. A. Mateos, S. Park, P. Leoni, B. Gheneti, F. Duarte, C. Ratti, and D. Rus, "Design, modeling, and nonlinear model predictive tracking control of a novel autonomous surface vehicle," in *2018 IEEE International Conference on Robotics and Automation (ICRA)*, pp. 6189–6196, IEEE, 2018.

[2] T. Shan, B. Englot, D. Meyers, W. Wang, C. Ratti, and R. Daniela, "LIO-SAM: Tightly-coupled lidar inertial odometry via smoothing and mapping," in *IEEE/RSJ International Conference on Intelligent Robots and Systems (IROS)*, pp. 5135–5142, IEEE, 2020.

[3] T. I. Fossen, *Guidance and control of ocean vehicles*. West Sussex PO19 1UD, England: John Wiley & Sons Ltd, 1994.

[4] J. Yu, J. Yuan, Z. Wu, and M. Tan, "Data-driven dynamic modeling for a swimming robotic fish," *IEEE Transaction on Industrial Electronics*, vol. 63, no. 9, pp. 5632–5640, 2016.